Geoderma, 51 (1991) 51–91
Elsevier Science Publishers B.V., Amsterdam

Quantitative geochemical approach to pedogenesis: importance of parent material reduction, volumetric expansion, and eolian influx in lateritization

George H Brimhall[a], Christopher, J. Lewis[a], Chris Ford[b], James Bratt[c], Gordon Taylor[c] and Oliver Warin[c]

[a]*Department of Geology and Geophysics, University of California, Berkeley, CA 94720, USA*
[b]*BHP Utah Mali Inc., B.P. 2856, Bamako, Mali*
[c]*BHP-Utah International Minerals, 550 California St., San Francisco, CA 94104, USA*

(Received November 15, 1989; accepted after revision August 15, 1990)

ABSTRACT

Brimhall, G.H, Lewis, C.J., Ford, C., Bratt, J., Taylor, G. and Warin, O., 1991. Quantitative geochemical approach to pedogenesis: importance of parent material reduction, volumetric expansion, and eolian influx in lateritization. In: M.J. Pavich (Editor), Weathering and Soils. Geoderma, 51: 51–91.

Using mass balance techniques we test the prevalent view that laterite genesis is dominated by in situ residual enrichment during chemical weathering of bedrock. Through calculation of net mass fluxes through the laterite soils in Mali, West Africa, we show that residual enrichment by removal of mobile elements with a corresponding increase in bulk porosity and decrease in bulk density, contributes only a very minor fraction of the enrichment of Al, Fe, Si and Au. Instead, we demonstrate that the abundance of these elements is due to the influx and accumulation by selective retention of chemically mature detritus of local and foreign origin clearly evident in micromorphological infilling features. At the same sample depths that accumulation reaches extreme values, we show that volumetric expansion in excess of 200% has occurred locally. We infer that these spatially coincidental zones of mass influx of rock-forming metals Fe, Al, Si, and also Au with dilational hyperstrains result from a mutually reinforcing, mechanical interaction between material influx and the effects of subsurface deformational processes such as shrink-swell cycles and root growth and decay. We propose that with progressive infilling of available connected voids by illuvial microsedimentary deposits of insoluble resistate and neoformed minerals, the capacity for the combined skeleton and plasma to remain isovulumetric is exceeded. We speculate that the resultant space problem is relieved by upwards expansion towards the overlying free surface. Continued translocation and void infilling occur and are limited to the depth where the size of translocational particles is smaller than that of the connected voids. Consequently, progressive hyperstrains accumulate above this critical depth by the long-term influence of a proposed translocational wedge of chemically-resistant minerals against which numerous generations of plant roots have exerted stresses.

Eclectic surficial contaminants involved are continuously derived from above leaving no indication of a relict source region within the present soil profile from which they might have been extracted. Instead, the source region is largely the existing regolith column itself which releases local material and in addition, is supplemented by deposition of colluvial detritus shed nearby by escarpment retreat

0016-7061/91/$03.50

and from contributions by foreign eolian sources. The regolith undergoes progressive reduction by wind deflation, erosion, local dissolution and reprecipitation. This open-system in situ fractionation process may be characteristic of tectonically-stable continental weathering in general where the relative stability of the landscape contributes to the accession, superficial recycling and retention of resistant minerals by interrelated mechanical, chemical and biological mechanisms. Residual enrichment in lateritic weathering profiles which has an increasingly-eclectic grain character near its top is then best viewed as only the first step of in situ modification of parent material. As such, residual enrichment dominates only the basal saprolitic portions of laterites but higher up is subordinate too the accumulated effects of translocation and accumulation of mineral detritus within voids. Lithostructure is progressively destroyed by bioturbation, mixing and expansion. The migration of surficial detritus into the ocean basins is thereby delayed and widespread cumulative lateritic soils become the long-term repositories of an aged continental residuum.

Gold is one mineral which is highly concentrated in the zone of lateritic weathering above mineralized Precambrian volcano-sedimentary greenstone protoliths and this surficial enrichment is of considerable economic importance. It appears that because of its small particle size and unusually high grain density, gold particles contained in the parent material are effectively enriched mechanically during regolith reduction as a captive constituent in the laterite column and are selectively separated from gangue constituents which are physically or chemically carried away by eolian and fluviatile regolith reduction and in solution in groundwater discharge.

INTRODUCTION

Laterites, including ferruginous tropical and sub-tropical Red Soils, presently mapped as Oxisols, Ultisols and Aridisols, broadly grouped together are estimated to cover as much as one third of all the emerged lands of the world (Nahon, 1989). The prevailing view of their origin is as being residual surficial accumulations of insoluble oxides and hydrous oxides of Fe, Al, Ti, Mn and silicate clays left in place and locally reworked while more soluble constituents are carried away in solution in groundwater. Since laterites are so widespread and occasionally extend to depths in excess of one hundred meters, they are perhaps as important globally as any known broad group of soils. Therefore, as a subaerial repository of relatively immobile chemical species, laterites affect a significant local hydrochemical fractionation of immobile from mobile chemical elements and thereby influence the composition of river discharge. On a larger scale, it is also likely that lateritization contributes to long-term changes in the chemical and isotopic character of the oceans when continental landmasses are subject to intense weathering within equatorial latitudes. Understanding of the relationship of widespread laterization to landscape evolution, paleoclimate, and continental drift is important for interpreting the long-term mass exchanges between continents and oceans. Further developments require knowledge of the age of laterites, duration of weathering processes, rates of conversion of bedrock to soil, surficial erosion rates and extent of eolian and fluviatile influx of locally-derived and foreign detritus into soils.

Global environment of laterites

By far the most expansive development of laterites is on tectonically-stable Precambrian cratonal continental masses. There, their accumulation as surficial products of intense chemical weathering of bedrock proceeds relatively undisturbed by removal of soil by active fluviatile erosion. The eventual passage into the oceans of chemically-mature debris created by lateritic weathering is hence delayed and its surficial residence time is prolonged. Rather than a dominance of erosive phenomena as on orogenic areas, the topographically-subdued landscape and its long-lived soil mantle may then contribute to a predominance of interrelated geochemical and biological processes including tree root heave, termite activity, and root dilation that cause a progressive reworking of detritus from surface to subsurface to surface again, recycling the most mature mineral constituents as well as nutrient cations used in the biochemical cycle. Furthermore, since global wind trajectories (Fig. 1) crossing cratonal areas emanate from hyper-arid and semi-arid interiors of continents where high dust-storm activity, wind erosion (Morales, 1979; Goudie, 1983; Pye, 1987) and desertification (El-Baz and Hassan, 1986) predominate, we hypothesize that deposition of dust of local or distant origin may contaminate laterites with chemically-mature detritus. Millions of tons per year of dust are carried from the Sahara and contribute to soils or oceans surrounding this desert region alone (Yaalon, 1987). Therefore, rather than view laterites as simple residual deposits, we examine them for possible foreign source material. Here, we first develop a new strategy for studying laterites in terms of their possible open geochemical system behavior.

Strategy

The choice of which properties of laterites to measure to offer essential genetic information is guided by a physical and chemical model which obeys the principle of conservation of mass (Brimhall et al., 1985) and incorporates a term expressing mass fluxes (Brimhall et al., 1988). With a mass balance approach we can use the chemical elements themselves as geochemical tracers. The behavior of tracer elements, both those which are immobile and mobile, is then interpreted in terms of formal mass balance principles presented as functional forms of constitutive relations between soil chemical composition, bulk density, porosity, and volume change in relation to similar properties of the parent material.

Our methods do not reject existing observational pedogenic techniques such as micromorphology or selective solvent extraction in favor of physio-chemical measurements. On the contrary, we continue to utilize them in studying

soils, but proceed to incorporate them into a more powerful quantitative strategy supported by general mass balance models in which all such field and microscopic observations, as well as mineral chemistry must fit with internal consistency and compatibility with bulk chemistry and physical properties. We hope therefore to offer an integrative compliment to existing pedological methods, which embraces direct observation and analytical measurement with physio-chemical models adapted for specific pedogenic systems.

Qualitative genetic model

Although excellent descriptions of laterites exist (Goudie, 1973; McFarlane, 1976; Butt, 1983; Golightly, 1981; Esson, 1983), their inferred origin is based largely on insightful, though often speculative, inference about past climates or climatic change for which there has been a scarcity of independent evidence. For example, isolated occurrences of laterite capping low hills in the Coast Ranges of Oregon and California have been rationalized by proposing past wetter climates in the Tertiary (Hotz, 1964; Cumberlidge and Chase, 1968). Elsewhere, climatic change to more arid conditions has been invoked to explain the apparent cessation of laterite formation by incision of drainage through duricrusts, escarpment retreat and redeposition of detritus in lowlands in yet younger weathering profiles (Goudie, 1973). The apparent geomorphic persistence of these old armored surfaces is explained by their relative resistance to erosion. A clear need exists to sort out the cause and effect relationships in chemical weathering, landscape evolution, climate, and tectonic stability. Rather than interpret lateritized terrains in terms of assumed climatic change, we wish to further develop the factual record here and then proceed to develop their use as paleo-climate indicators subsequently.

On the small scale of weathering profiles, laterite genesis from bedrock parent material is generally conceptualized as a spontaneous development of vertically-zoned and differentiated soils in response to intense tropical weathering of a variety of igneous, sedimentary and metamorphic bedrocks (Nahon, 1989). At their base, advance of the weathering front proceeds at the expense of parent rock as percolating groundwater carries away soluble constituents leaving the remaining saprolite enriched in relatively insoluble species but essentially intact structurally as original rock texture is preserved. However, in addition to the profiles developing from the base upward in this fashion, they also mature from the top down by intense pedogenic modification and may as well receive influx of detritus of local and distant origin of a chemical maturity characteristic of surficial exposures in the source region. Thus lateritic weathering is simultaneously induced both from below and above by advance of two very different processes; one at depth affecting incipient alteration of bedrock apparently under water-saturated reducing conditions, and the other completing a progressive evolution in chemistry, structure, and physical properties, which has proceeded downward by replacement of each

zone by its superadjacent and pedogenically more mature counterpart leading towards complete oxidative equilibrium with the atmosphere. Thus, the zonal sequence is a series of dynamic partial equilibrium states between the solid earth and the atmosphere, mitigated by the migration and reactivity of percolating groundwater and ground gasses.

The uppermost portions of laterites vary considerably and include Oxisols and Ultisols. Frequently, capping laterite profiles are indurated duricrusts of concretionary pisolitic ferricrete (Tardy and Nahon, 1985) referred to as hardpans or canga, forming topographic mesas separated by flat lowlands. Such features are believed to show their considerable age and progressive development of each horizon from a progenitor which resembled that currently underlying it (Butt, 1983). Local enrichment of low-level laterites by detritus shed from nearby high-level laterites is inferred from the fragmented nature of hardcaps near the edges of mesas where tree roots often occupy cracks between disoriented blocks and the occurrence of hardcap inclusions in younger duricrusts below.

In the West African, Brazilian, and Guyanan shields, surface denudation rates of 10–50 m/Ma are so slow that erosion is transport limited, as the rate of supply of material by weathering exceeds the capacity of transport processes to remove the material (Stallard, 1989). Under such conditions, weathering penetrates to depths exceeding 40 m and is relatively complete. The resultant lateritic soils (Oxisols, Ultisols, and Ferrisols) and derivative suspended sediments in rivers contain Na, K, Mg, and Ca cation-depleted minerals principally silicate clays and Al–Fe sesquioxides. This mineral suite is chemically more mature than that typically derived from erosion in tectonically-active mountain belts where denudation rates are rapid, in the range of 50–5000 m/Ma and alumino-silicate rocks do not weather so completely.

Metallogenesis

Though generally poor in many plant nutrients, laterites are soils of considerable agricultural and economic importance particularly in many developing countries in Africa, India and South America. Of growing importance in these areas is the considerable mineral resource potential of laterites which already constitute a significant portion of the world's Al, Ni, and Co reserve. Laterites are also the focus of an intense regional exploration for Au sparked largely by the discovery of the huge Boddington gold-enriched laterite in Western Australia developed by weathering of a gold-bearing volcan o-sedimentary greenstone protore of the Archean Yilgarn craton (Davy and El-Ansary, 1986). Enrichment mechanisms for gold involving ferrolytic oxidation of ferrous Fe during precipitation of goethite have been proposed (Mann, 1983a, b, 1984; Webster and Mann, 1984), directly linking chemical gold enrichment to lateritic weathering.

The metallogenic significance of lateritic weathering is immense both for metals and industrial minerals. Regional dust trajectories (Fig. 1) emanating from the arid continental interiors may contribute to further enrichment of in situ bauxite deposits of Al (Brimhall et al., 1988). Submarine clay plumes in seafloor sediments represent the distal sites of offshore dust deposition. Nearer to the continental source regions, but still positioned along dust trajectories, coarser-grained, clastic terriginous sediment collects in proximal shoreline environments as heavy mineral beach sand deposits representing most of the world's mineral resources of Zr and Ti. Together, these varied mineral deposits from widespread fractionation sequences of continental detritus distributed hydrodynamically along dust trajectories (Brimhall et al., 1988).

Therefore, as a widespread group of residual soils which also includes bauxites, laterites have been intensively studied as major global sources of Ni, Co, and Al and more recently intensively explored internationally for enriched Au, Pt and Pd ore deposits. Because of the many difficulties of successfully exploring in deeply-weathered terrains where bedrock geology is obscured (Smith, 1983) and interpretation of leached outcrops is complicated, the tremendous global resource potential of these soils is only now being realized with application of rapid advances in multi-element regional geochemical sampling methods. While proving to be effective in locating gold-enriched laterites, regional geochemical mineral surveys in these poorly-exposed and deeply weathered laterized terrains have accentuated the need for an improved general understanding of laterite genesis, age, geochemical dispersal patterns and response to climatic change. Thus, knowledge of the response of many valuable and geochemically-diverse transition metals to complex pedogenic processes then becomes vital to mineral exploration.

PURPOSE OF THIS STUDY

The purpose of this paper is to illuminate the chemical mass exchanges between vertically adjacent pedogenic compartments within laterites and to relate this mass transfer to surficial processes. Mechanistically, this amounts to establishing the extent of open-system transport in a deforming porous media, a task which has in the past been impeded for lack of a means of evaluating the state of strain so that chemical gains and losses should be calculated accurately. Physical strain markers are often scarce making it necessary to devise a more general technique of estimating strain. Using Zr and Ti, two elements which are viewed as being relatively immobile, we study their behavior quantitatively in order to evaluate strain as rigorously as possible. This done, we establish mass influx of major soil-forming elements: Al, Fe and Si, turning lastly to Au behavior as an important ore metal enriched in laterites,

as well as being unique in its property of density which make it a particularly revealing tracer constituent mechanically.

THEORY OF GEOCHEMICAL MASS BALANCE

Background

The derivation and application of constitutive mass balance techniques to hydrochemical weathering processes are described in detail by Brimhall et al. (1985), Brimhall and Dietrich (1987), and Brimhall et al. (1988). The term constitutive is used simply because we have derived formal analytical relationships between physical and chemical properties of soils in relation to their parent material under constraints imposed by conservation of mass. Of greatest importance, however, is that these constitutive relations are explicit functional forms from which interpretation of distinct pedogenic processes becomes possible. From our previous experience applying mass balance analysis, we now have a useful strategy at our disposal with which to address open-system soil development.

Complexity of determining elemental mobility

Our purpose in this section is to develop a set of analytical mass balance functions which, when applied to sets of chemical and physical data, can be used to determine open chemical system gains and losses in soil profiles in relation to their parent material. The transformation of parent material to soil is due to the action of a complex combination of interrelated surficial processes that include hydrochemical, biological, mechanical and eolian factors. To succeed in unraveling such complex patterns, we must require that models accommodate the complexity of the near-surface environment of lateritic weathering. This entails evaluating all assumptions and limitations in light of specific field circumstances and petrographic observations.

Basic conservation equation

The basic constitutive equation expressing the overall conservation of mass of any chemical element, j, relates volume, dry bulk density, and chemical composition and mass fluxes into or out of the system:

$$\frac{V_p \rho_p C_{j,p}}{100} + m_{j,\text{flux}} = \frac{V_w \rho_w C_{j,w}}{100} \qquad (1)$$

The first term on the left-hand side of eq. (1), expresses the mass of element, j, contained in the protolith before weathering, subscripted as p. It is given by the product of volume (V in cm^3), dry bulk density (ρ in g/cm^3), and chem-

ical concentration (C in wt%). Notice that the units combine to give the mass of element j in grams. The mass of element j introduced into or out of the protolith volume is indicated as $m_{j,\,\mathrm{flux}}$ and is added to the mass of j in the protolith. Fluxes are taken as positive if they come into the system and are negative if they leave the system. On the right-hand side of eq. (1), the mass of element j contained in the weathered product volume of interest, subscripted w, is given by the product of the new volume, dry bulk density, and chemical concentration.

Meaning of volume: the sample system

The concept of volume used in this context refers to representative elementary volumes, abbreviated REV. For a homogeneous starting material, a REV can be quite small, and field samples of 100 cm^3 are equivalent and can be conveniently taken in soil profiles. The mass conservation equation then applies to *individual sample volumes* with the boundaries of each chemical system being their outside surface.

Volumetric strain

We make no assumption about chemical and biophysical weathering being isovolumetric and seek instead to determine volumetric changes. We accomplish this by utilizing the classical definition of strain, ε, the ratio of volume change in a process to the initial volume:

$$\varepsilon_{i,\,w}=\frac{V_w-V_p}{V_p}=\frac{V_w}{V_p}-1 \tag{2}$$

Subscript i refers to the strain determined by use of an immobile strain index element and subscript w refers to strain due to weathering. Notice on the right-hand side of eq. (2) that the strain can be expressed as a ratio involving V_w/V_p. Rearranging eq. (2) shows that strain is a unitless ratio:

$$\frac{V_w}{V_p}=\varepsilon_{i,\,w}+1 \tag{3}$$

Note that the volumes denoted in eqs. (1–3) are representative elementary volumes (REV) of sufficient size so as to be homogeneous throughout. In most cases, a hand-sample size is sufficient to insure homogeneity.

Mass fluxes

Since we are primarily interested in open-system mass fluxes, we solve eq. (1) for $m_{j,\,\mathrm{flux}}$:

$$m_{j,\,\mathrm{flux}}=\frac{V_w\rho_w C_{j,w}}{100}-\frac{V_p\rho_p C_{j,\,p}}{100} \tag{4}$$

and divide by V_p to give eq. (5) which contains V_w/V_p ratios which we can soon eliminate using eq. (3), replacing them by $\varepsilon_{i,\,w}+1$:

$$\frac{m_{j,\,\mathrm{flux}}}{V_p}=\frac{V_w\rho_w C_{j,\,w}}{100V_p}-\frac{\rho_p C_{j,\,p}}{100} \tag{5}$$

Substituting in $\varepsilon_{i,w}+1$ from eq. (3) for V_w/V_p gives the mass flux relative to the volume of the protolith:

$$\frac{m_{j,\,\mathrm{flux}}}{V_p}=(\varepsilon_{j,\,w}+1)\frac{\rho_w C_{j,\,w}}{100}-\frac{\rho_p C_{j,\,p}}{100} \tag{6}$$

Mass transport function

Although this volume reference for the fluxes could be used, it is preferable instead to relate fluxes to the mass of element j contained in the original protolith. In order to compute the fluxes in this fashion, we define the open chemical system transport function, $\tau_{j,w}$ as the mass fraction of element j added to the system during weathering relative to the mass of j originally present in the protolith. This is the product of V_p and $C_{j,p}\rho_p$:

$$\tau_{j,\,w}=100\frac{m_{j,\,\mathrm{flux}}}{C_{j,\,p}\rho_p V_p} \tag{7}$$

Calculation of the open system mass transport function, $\tau_{j,\,w}$

Solving eq. (7) for $m_{j,\,\mathrm{flux}}$, substituting the resultant expression into eq. (6), and dividing by $\rho_p C_{j,\,p}$ gives eq. (8). This is the form of the open-system mass transport function, or mass fraction added or subtracted, we use to compute chemical gains and losses for each sample collected from a soil profile. Hence we compute $\tau_{j,\,w}$ directly from density and chemical composition data in combination with interpreted strain:

$$\tau_{j,\,w}=\frac{\rho_w C_{j,\,w}}{\rho_p C_{j,\,p}}(\varepsilon_{i,\,w}+1)-1 \tag{8}$$

Briefly, $\tau_{j,\,w}$ values of -1.0 signify that 100 percent of the mass of element j originally present in the protolith has been extracted during weathering. A value of 0.0 indicates that the element has been immobile and has been affected only by internal closed chemical system processes, specifically, residual and strain effects. This does not imply that other elements have been immo-

bile, however, and they may be part of the open system. Finally, a positive value of $\tau_{j,w}$, for example 0.5, means that an excess of 50 percent of the mass of element j has been added.

Determination of strain

In order to compute the transport functions for each element of interest, it is necessary to first compute strain. This can only be done by use of an immobile element. Alternatively, certain geometric relationships such as vein patterns serving as physical strain markers could theoretically be used, but they are present so rarely, especially above the saprolite, that they are of little practical use. Several elements are almost certainly immobile under most near-surface geological circumstances. Zr and Ti are perhaps the most immobile of all as the minerals zircon and rutile are generally quite insoluble in groundwater, though not universally so. To compute strain, we assume that an element like Zr has been immobile. It follows then that the flux term in eq. (7) is zero, and hence the open-system transport term $\tau_{j,w}$ in eq. (8) is also zero. Therefore, if an element is in fact immobile, eq. (8) can be rearranged to yield eq. (9) where subscripts j have been replaced by i to indicate an immobile element:

$$\frac{\rho_w C_{i,w}}{\rho_p C_{i,p}}(\varepsilon_{i,w}+1)=1 \tag{9}$$

Solving eq. (9) for strain gives eq. (10) which is the form we use to compute strain due to weathering for each field sample:

$$\varepsilon_{i,w}=\frac{\rho_p C_{i,p}}{\rho_w C_{i,w}}-1 \tag{10}$$

Correct application of the technique depends upon establishing the existence of a homogeneous protolith and immobility of at least one chemical species, typically Zr or Ti, for use as the index species, i, in strain determination. In eq. (10) we see immediately that strain can result whenever a change in bulk density, ρ_w, is not exactly compensated by an inversely proportional change in the concentration of the immobile element, $C_{i,w}$ such that their product in the denominator remains constant and equal to the numerator with a value of unity. Certain types of strains are easily visualized using eq. (9), Imagine root dilation as an example. Because roots typically have a bulk density and a concentration of immobile elements such as Ti or Zr less than in rocks, the product $\rho_w C_{i,w}$ would clearly be less than the product for the protolith in the numerator. The overall quotient would be significantly greater than 1 so that with subtraction of 1, and shown in eq. (10), the resultant strain would be positive and hence dilational. Conversely, collapse by intense

dissolution of minerals containing mobile elements would leave the weathered product enriched in immobile elements contained in chemically-resistive minerals. Without a compensating change in density, the calculated strain would be negative consistent with collapse.

Calculation of gains and losses

By solving eq. (7) for $m_{j,\mathrm{flux}}$, we see immediately how mass fluxes for *each sample* system can be calculated using the open chemical system transport function:

$$m_{j,\mathrm{flux}}=\left(\rho_p V_p \frac{C_{j,p}}{100}\right)\tau_{j,w} \tag{11}$$

Within parentheses is the mass of element j contained in the protolith given as the product of bulk density, volume and concentration. By multiplying this original mass by the open-system transport function $\tau_{j,w}$ which is the mobile mass fraction, the resultant product gives the mass of j flux.

This gives the mass flux for a single sample of volume, V_p. What is generally more useful, however, is knowledge of an overall or net mass flux for an entire soil profile down to the depth investigated.

Overall mass flux of a profile, $\bar{m}_{j,\mathrm{flux}}$

This is accomplished by simply recognizing that since we can compute a value of $\tau_{j,\mathrm{flux}}$ for each individual sample, we can express $\tau_{j,\mathrm{flux}}$ as a function of depth, Z, down through the profile. $\tau_{j,\mathrm{flux}}(Z)$ may be integrated as a function of depth to the depth over which the profile has been sampled, $D_{j,w}$ or any depth of interest. We then calculate the overall or net mass flux, $\bar{m}_{j,\mathrm{flux}}$, for the entire soil profile to the depth $D_{j,w}$, as given by:

$$\bar{m}_{j,\mathrm{flux}}(\mathrm{g/cm^2})=\rho_p \frac{C_{j,p}}{100}\int_{Z=0}^{Z=D_{j,w}} \tau_{j,w(Z)}\,dZ \tag{12}$$

In eq. (12) we have expanded the REV term, V_p, in eq. (11) as the product of a depth, $D_{j,w}$, to which the flux is calculated and the cross-sectional area in plan view of the profile. This area has been moved to the left-hand side of the equation giving the units of grams per square cm. For example, if a profile had been leached of an element j to a depth of 2 m and had an average $\tau_{j,w}$ of -0.5, a protolith density of 2.6, and a concentration of j 0.4%, the average mass loss of element j per cm^2 of soil cross section would be 1.04 g to the depth of 2 m. The utility of the planimetric areal reference for these fluxes

can be appreciated by considering overall mass balance and weathering rates in drainage systems including transport in stream discharge (Velbel, 1985).

Mass fluxes in chemically-differentiated soil profiles

In certain chemically-differentiated soils such as Spodosols, there may be depth intervals over which the function, $\tau_{j,\,\mathrm{flux}}(Z)$, is positive, zero or negative. For example, consider the losses of Al or Fe in the albic zone in relation to the corresponding gains in the spodic zone. Mass fluxes can be computed individually for each zone using appropriate depth limits of integration in eq. (12).

Internal chemical changes

We turn now to separating open-system mass transport from two processes which can be visualized as being largely, though not uniquely, internal in origin in contrast to external processes which either introduce foreign material or carry constituents away in solution or suspension. The principal internal processes are residual enrichment and strain effects. A common method of expressing overall chemical enrichment is by using the enrichment factor, which is the ratio of the chemical concentration of an element divided by the concentration of that same element in the protolith. If the enrichment factor equals 1 than there has been no enrichment. If it equals 2, then the concentration is twice s high as in the protore. However, this does not mean necessarily that twice as much mass of element j has been added from external sources as internal enrichment processes may be sufficient to explain increase in concentration. Equation (6) is solved for an enrichment factor, $C_{j,\,\mathrm{w}}/C_{j,\,\mathrm{p}}$:

$$\frac{C_{j,\,\mathrm{w}}}{C_{j,\,\mathrm{p}}} = \underbrace{\frac{\rho_{\mathrm{p}}}{\rho_{\mathrm{w}}}\frac{1}{(\varepsilon_{j,\,\mathrm{w}}+1)}}_{\substack{(1)\\ \textit{closed system}}} + \underbrace{100\,\frac{m_{j,\,\mathrm{flux}}}{C_{j,\,\mathrm{p}}\rho_{\mathrm{w}}V_{\mathrm{p}}(\varepsilon_{i,\,\mathrm{w}}+1)}}_{\substack{(2)\\ \textit{open system}}} \qquad (13)$$

This equation represents two distinct contributions to the enrichment factor of each sample volume referred to here as the "closed" and "open" system parts labeled as terms 1 and 2, respectively. These will be discussed in order and related to the overall enrichment factor. The enrichment factor has considerable geochemical appeal as it represents change in composition in relation to the original concentration in a protolith. It therefore automatically normalizes analyses, both in terms of composition and density. Each of the terms in eq. (13) are therefore dimensionless ratios being scaled perfectly to initial properties of the protore.

Closed-system enrichment

The first term in eq. (13) describes the elements which behave as immobile constituents during weathering, and hence, the system is closed with respect to them while being open with respect to mobile elements. The contribution of immobile elements to the overall enrichment factor is a product of the density ratio of the protore to that of the weathered material divided by a second factor, the strain due to weathering plus 1. The density ratio is the part of enrichment referred to as residual. Residual enrichment results from dissolution and removal of mobile elements with a corresponding reduction in bulk density and a corresponding increase in porosity (Brimhall and Dietrich, 1987) with no reference to change in volume, as volume change does not necessarily follow and is expressed by a separate factor.

While transformation of bedrock to soil involves the release and transport of mobile elements out of the system, elements which remain behind are residually enriched. In eq. (13) the term with strain plus 1 in the denominator is a function of the amount of deformation due to weathering. It is important to realize that strain can have this effect of inducing enrichment. However, remembering that dilation corresponds to positive strain and collapse to negative strain, the fact that the strain term in eq. (13) appears in the denominator means that only the latter will cause enrichment.

Open-system enrichment

The second term in eq. (13) refers to the open chemical system and involves the mass influx or departure of element j. The greater the mass influx of a mobile element, then the greater the contribution to the enrichment factor for that element. It is clear from eq. (13) that the open-system component of enrichment adds directly to the closed-system component. By solving eq. (7) for $m_{j,\,\mathrm{flux}}$, substituting this expression into eq. (13), and factoring out the density ratio and strain functions, we can express the enrichment factor finally as:

$$\frac{C_{j,\,\mathrm{w}}}{C_{j,\,\mathrm{p}}} = \underbrace{\frac{\rho_{\mathrm{p}}}{\rho_{\mathrm{w}}}}_{\substack{\textit{residual}\\ \textit{enrich-}\\ \textit{ment}}}\ \underbrace{\frac{1}{(\varepsilon_{i,\,\mathrm{w}}+1)}}_{\textit{strain}}\ \underbrace{(1+\tau_{j,\,\mathrm{w}})}_{\substack{\textit{open}\\ \textit{system}}} \qquad (14)$$

For a given element, j, eq. (14) reflects the interactive effects of its closed-system (immobile) and open-system (mobile) constituent contributions to the overall enrichment factor. The open-system term refers to the constituents which move across the boundaries of the system and are therefore mobile. When there are no mobile constituents, mass influx $m_{j,\,\mathrm{flux}}$, equals zero and $\tau_{j,\,\mathrm{w}}$ equals zero. The enrichment factor is then simply the closed-system

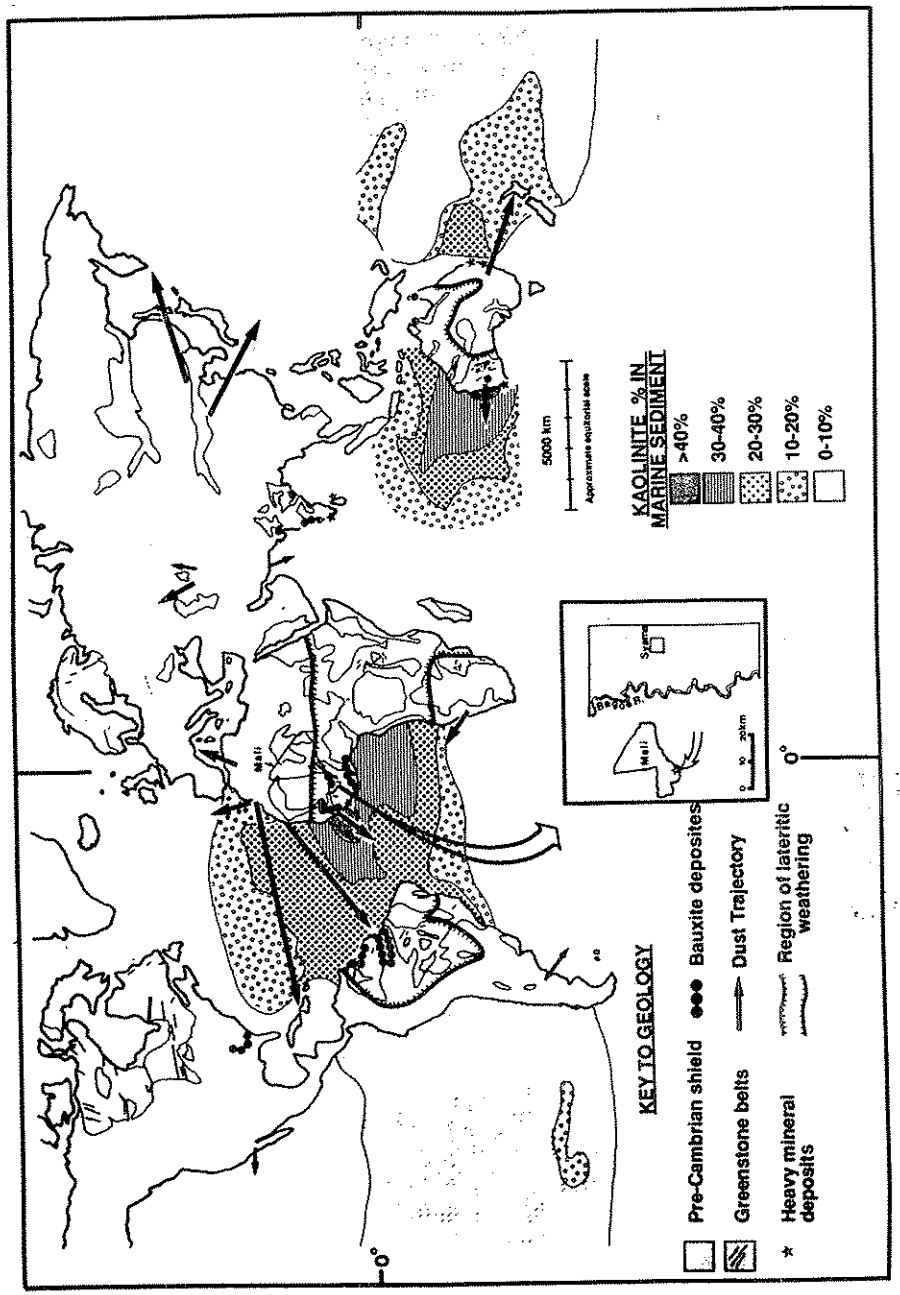

product of the density ratio times the strain term. The value of $\tau_{j,w}$ can, in addition to being equal to zero, be positive for additions of material or negative if material leaves the system. If $\tau_{j,w}$ equals 1 for example, then the enrichment factor is equal to two times the density ratio times the strain term. This corresponds to 200% of the mass of element j in the protolith.

Limitations of the method

Although the mass balance method allows useful inferences to be made about the involvement of pedogenic material from internal versus external source regions, one of its limitations is that it does not discriminate between in situ, or parautochthonous, and external, or allochthonous, sources. Secondly, since mass balance analysis uses characteristics of the protore as part of the computation of open system enrichment components, the accuracy with which projections of such properties can be made influences the accuracy of our conclusions about chemical gains and losses in a major way. Obviously, our method works best if the protore is as homogeneous as possible and when we have ready access to the parent material. In deeply-weathered terrains, the latter condition commonly requires diamond drill cores to characterize the protolith as soil pits deeper than 25 m are very rare.

FIELD STUDY SITE

In Africa, laterites occur within a wide belt of latosols spanning the equatorial regions within 20 degrees north and south latitude. We chose a study site at Syama in southernmost Mali, West Africa, 20 km east of the Bagoe River (Fig. 1). Our study site at Syama was chosen as it affords ideal opportunities in several respects. First, laterite profiles can be sampled from top to bottom, including unweathered parent material made available in exploration diamond drill core. Second, the site is positioned along a regional dust trajectory of the Harmatan winds, which provides an opportunity to determine what the level of incorporation of allochthonous detritus is into the laterites. Third, 15 m deep exploration pits could be easily sampled using piston coring methods. Fourth, as a lateritic gold ore deposit, the occurrence of particulate gold in the Syama laterites provides an opportunity to determine how mineral grains which are clearly autochthonous behave during regolith reduction; they are physically captive in the soil because of their exceptionally high density and hence not susceptible to wind ablation.

Fig. 1. Global map showing Precambrian shields (Derry, 1980), submarine lava greenstone belts (De Witt et al., 1988), laterite distribution in Africa (Goudie, 1973), ferricrete distribution in Australia (Goudie, 1973; and other sources: BHP-Utah International internal reports), lateritic bauxites (Valeton, 1983), heavy mineral beach sand deposits (Dixon, 1979), global dust trajectories emanating from arid and semi-arid regions (Pye, 1987), kaolinite-enriched marine sediments (Pye, 1988), and location of study site in Mali, West Africa.

Bedrock parent material

The bedrock at Syama is a hydrothermally-altered submarine lava or greenstone, probably originally a chloritized basalt which upon later mineralization was enriched in gold. The accompanying alteration assemblage includes quartz, albite, ferroan-dolomite and minor white mica controlled by veinlets containing quartz, graphite, auriferous pyrite, chalcopyrite, trace electrum and quartz. The quartz sometimes shows pressure shadows due to intense deformation. Structurally, the bedrock is a sequence of moderately steeply-dipping metamorphosed Birimian volcano-sedimentary rocks approximately 2 billion years old. Similar Precambrian greenstone belts occur as linear fault-bounded grabens in the major Precambrian shields of West Africa, Canada, Australia, and Scandanavia (Fig. 1).

LATERITE WEATHERING PROFILES

Sampling

We offer here completed results on our research efforts studying 14 piston core soil samples taken in January 1988 from a 15 m deep, 1 m^2 cross-section exploration pit at Syama. The pit is referred to as SP-15 and samples from it are collection number 1147. Pit SP-15 was sampled using a hand-held sliding hammer piston coring device which takes two 7.6 cm long cores, 4.7 cm in diameter which are sheathed in durable Lexan plastic tubes (Fig. 2) each with a volume of 132 cm^3. The tubes are capped to retain soil moisture, thereby providing oriented samples for chemistry, physical properties, hydraulic conductivity, and micromorphology.

Nearby diamond drill core samples from hole SYD-4 (our sample collection number 1149) were considered as representative of the fresh protolith (protore) or parent material from which laterites developed. Diamond drill core samples were taken at inclined drill hole depths of 65.7, 86.1, 94.8, and 100.8 m which have projected vertical depths below the surface of 46, 60, 66, and 70 m, respectively. In our calculations, these protore samples provide the initial state of mineralization upon which all subsequent weathering effects are assumed to have taken place.

Physical properties

The greenstone bedrock has been weathered to a vertically-zoned sequence beginning with saprolite above the bed-rock weathering interface (Fig. 3). Above this, the mottled zone or carapace and hardcap, locally referred to as the cuirasse, occur in sequence capped by non-indurated gravels. In Figs. 3a–3c we show the variation in bulk dry density, average mineral grain density

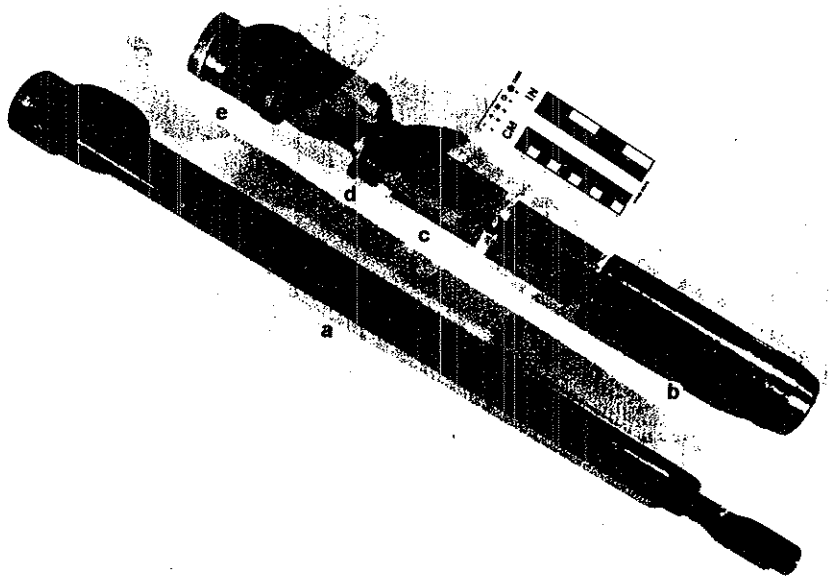

Fig. 2. Hand-held piston hammer soil sampler (a) and parts: sharpened steel cylinder cup penetrometer (b), Lexan plastic core barrel inserts (c), threaded cylinder cap (d) which attaches to end of (a), and example of a capped soil core (e). Sampler is available through Art's Manufacturing (AMS), 105 American Falls, Idaho 83211.

and porosity for 14 samples from pit SP-15 (1147-1 to -14) and 4 core samples or grant material (1149-1 to -4). The most notable trends in these profiles with depth are the decrease in bulk dry density and dramatic increase in porosity from 30 to over 60%. Major changes in pore structures occur over the depth of 15 m. Near surface, in the carapace, many large macroscopic voids occur which lower the bulk density to well below that of the protore. However, at depth, within the saprolite, the voids are much smaller, typically at a submicron level, but more numerous. This lowers the bulk density still farther. This marked change in pore structure frequency and size has a significant impact on the saturated permeability of the profile. In Fig. 4 the saturated hydraulic conductivity of soil cores undergoes an abrupt drop from 0.001 cm/s to less than 0.00001 cm/s at a depth of about 13 m within the saprolite. This transition from microscopic to submicroscopic pores represents a reduction of between 1/100 and 1/1000 of the hydraulic conductivity higher in the profile.

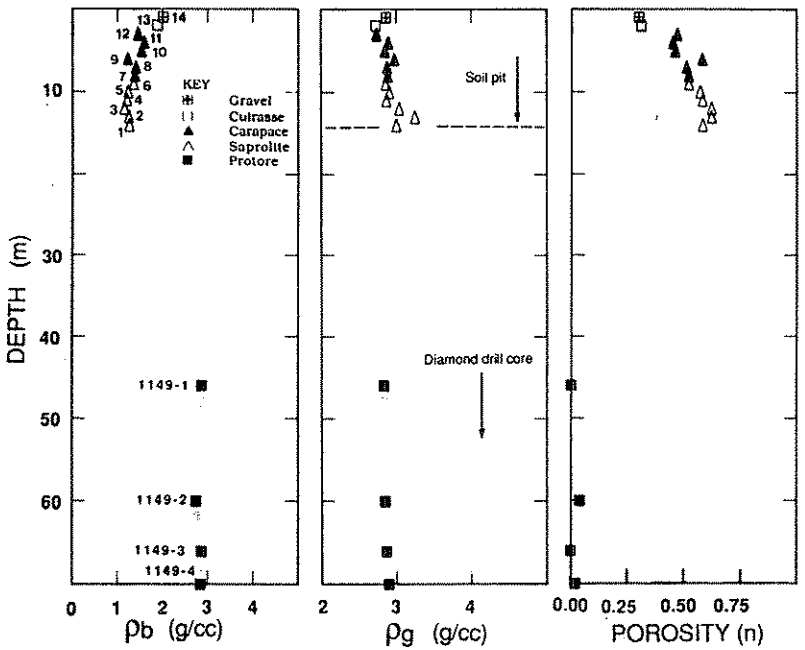

Fig. 3. Physical property profiles of soil pit SP-15 at Syama: bulk dry density (ρ_b), average mineral or grain density (ρ_g), and calculated porosity (n) derived from the equation, $n = 1 - \rho_b/\rho_g$. Depth of sample pit is shown in comparison to position of diamond drill hole (D.D.H. SYD-4) core samples of parent material.

Strain calculation from chemomechanical indicators

In order to determine the chemical gains and losses of elements that have occurred along with physical changes during weathering, it is first necessary to ascertain the state of strain of the deformed porous media. Secondly, recall that in order to determine the net strain, we must identify and use an immobile element in a closed-system constitutive mass balance relation (eq. 10) which relates strain to bulk density and concentration. This conceptual constitutive relation approach departs markedly from well-known statistical factor analysis methods (Esson, 1983) which (1) normalize multi-element chemical data to immobile index species, and (2) assumes that Zr and Ti, which are the usual choices for these immobile elements, have not been introduced into the profile. Here, instead of relying on empirical normalization or on the assumption of immobility of index species, as do past studies, our strategy specifically addresses the mobility of each element as independently as possible. Also, we directly determine if introduction of minerals containing

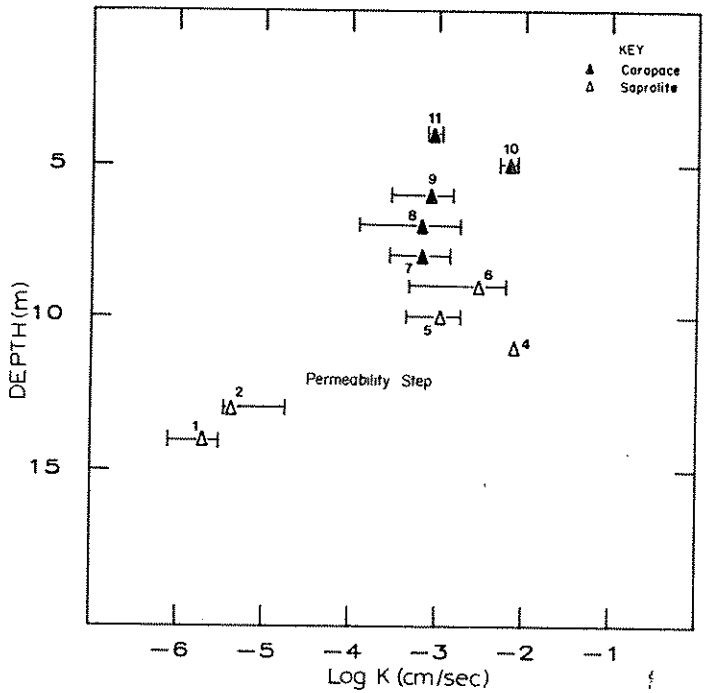

Fig. 4. Saturated hydraulic conductivity measured on soil cores placed in a permeameter fitted with multiple manometers from which the hydraulic gradient can be measured directly and used to solve Darcy's law for hydraulic conductivity.

so-called immobile elements has occurred. Serious errors in mobility patterns of all elements can result if an index mineral has in fact been introduced into a profile. Finally, physio-chemical mass balance techniques also are much easier to understand than the procedural steps in previous soil development analysis (Barshad, 1964).

It is worth examining the reasons for the traditional focus in pedogenic studies on Zr and Ti as possible immobile elements. It is based upon several lines of reasoning. The fact that these elements, often accompanied by Al, Nb and V are commonly enriched in the B horizon, where they reach levels many times their concentrations in bedrock (Esson, 1983), is essentially due to the relative chemical stability, as evidenced by the preservation of their host minerals in sediments or resistance to weathering (Lelong et al., 1976; Birkeland, 1974; Samama, 1986). The underlying reason for the stability of minerals like rutile, however, comes directly from electronic structure of transition metals in the Periodic Table. Oxides of these metals have standard state enthalpies of formation from the elements which increase systematically from

left to right across groups within a given period of the Periodic Table as d-orbitals are successively filled (Brimhall, 1987). The most stable, and hence least soluble minerals, are those with the lowest enthalpy. These are minerals containing Ti, Zr, Y, Nb, which are on the left side of the transition metals.

Another line of reasoning used to infer that these elements are immobile is that the ratio of their concentration sometimes does not vary substantially throughout a soil profile, implying that they are a "residual" component of soils. This assumption about constancy of concentration ratios indicating immobility can be erroneous simply because all a constant ratio really shows is that the two elements have behaved more or less the same, not that they have been immobile, as they may have been introduced or removed in step.

Introduction and translocation of zircon

In order to identify useable immobile elements, it is therefore necessary to demonstrate that the principal minerals containing them are immobile or, if introduced from an external source or by reduction of the regolith volume, an accurate correction must be made to the total chemical concentration profiles, by deducting the mass of the element translocated, thereby yielding the mass concentration of immobile elements. Several recent studies have addressed mechanical migration of accessory minerals which are relevant to this

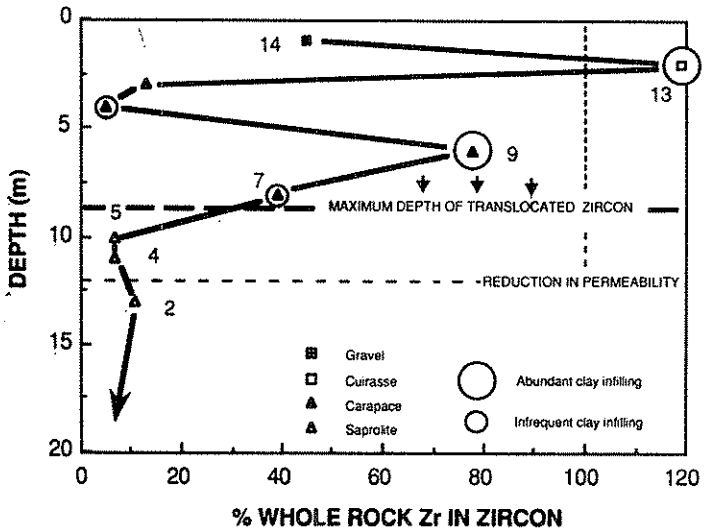

Fig. 5. Contribution of zircon to the total Zr content of samples. High precision modal analysis (Brimhall and Rivers, 1985) is performed on HF acid partial digestion residues. Zr chemistry is by XRF on pressed pills using a cellulose binder. Extent of micromorphologic infilling structures are indicated and reach maximum values in samples 9 and 13.

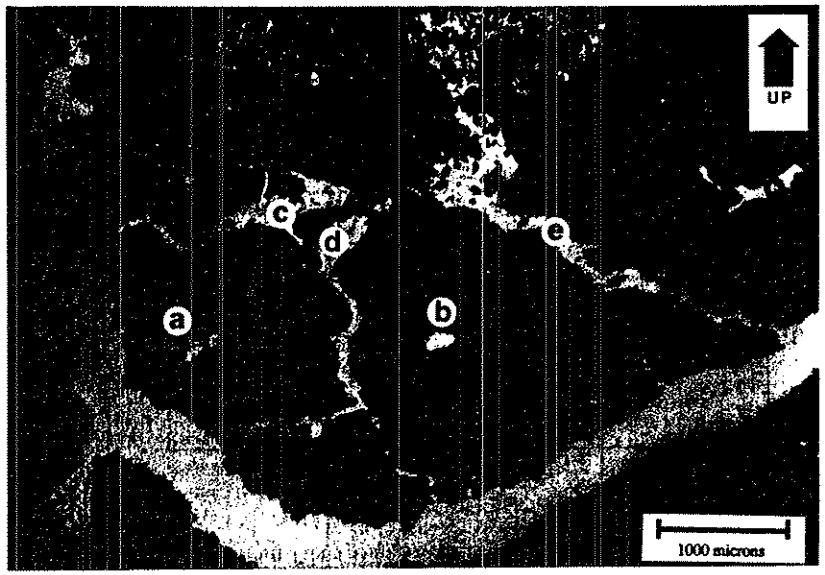

Fig. 6. Photomicrograph showing cumulative soil texture with numerous generations of clay infilling in their true orientation as indicated by 'up' arrow. Progressive development of pores is evident in modern, partially-open pores (*a* and *b*) which onlap and cross-cut older infillings above microsedimentary unconformities. Artificial dessication cracks induced during sample drying in the laboratory are shown in *c*, *d* and *e*.

problem (Davy, 1979; Brimhall et al., 1988). Here, we have made partial acid digestions of samples in hydrofluoric acid which dissolves soluble minerals and leaves a residue of zircon and rutile.

We have shown previously that the acids used do not attack zircon and leave the morphology of zircon and rutile unchanged (Brimhall et al., 1988). The volumes of the remaining acid-resitent minerals have then been accurately measured on a digitizing microscope (Brimhall and Rivers, 1985). Figure 5 shows the amount of wholerock Zr accounted for by rounded zircon remaining in the acid residues. Since the parent material does not contain recognizable zircon, Fig. 5 shows the amount of translocated zircon introduced from the top of the profile. The depth to which this translocation reaches is limited to 8 m. Less than 1% of the total titanium content of the soils occurs as rutile, indicating that the titanium profile need not be corrected for translocation.

Besides clear cut evidence of zircon translocation, micromorphology reveals that there is ample evidence of translocation and accumulation of silicate clays and iron oxide phases as well (Fig. 6) with crescentic clay film infillings in pores. The abundance of clay pore infillings is shown in Fig. 5,

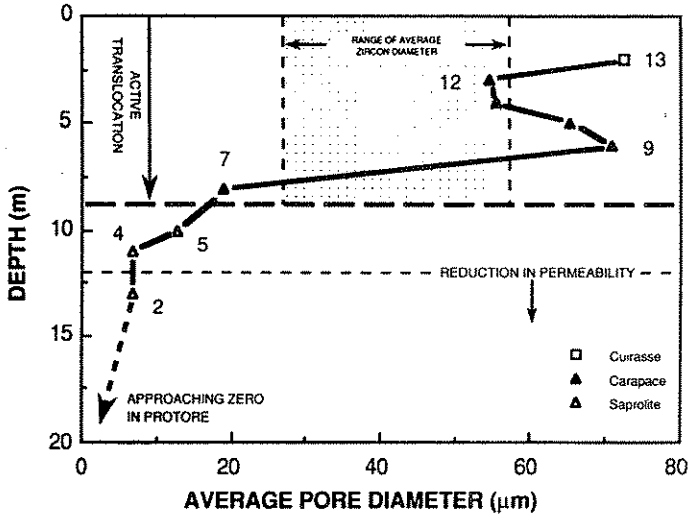

Fig. 7. Average diameter of pores as measured in stained epoxy-impregnated thin sections using digitizing microscope of Brimhall and Rivers (1985) which highlight modern pores structures. Average size range of detrital zircon is shown, and exceeds the size of pores below 8 m depth.

indicating a close correspondence of the amount and maximum depth of zircon and clay translocation. Both introduced constituents are limited to the upper 8 m, a depth which is only slightly above the permeability step at 12 m. The physical explanation why translocated zircon is limited to the upper profile is evident in Fig. 7, where we show that zircons with an average size range within each sample of 30 to 60 microns, are simply too large to fit through available pores below a depth of 8 m where the average pore diameter decreases from over 60 microns to less than 20 microns.

Zr profile corrected for translocation

A Zr profile corrected for translocated zircon (Fig. 5) is shown in Fig. 8 (left panel) juxtaposed with an uncorrected Ti profile requiring no correction as rutile translocation is negligible. Notice for that samples 7, 8, 9, 13 and 14, the corrected Zr concentration is appreciably lower than the uncorrected assay. Sample 5, is anomalously rich in Ti, a fact we attribute to that interval containing a vein structure rich in Au as well as Ti.

Strain profiles

Strain profiles using Zr and Ti, the former corrected for zircon translocation, are shown in Fig. 9 (left and right panel, respectively) calculated using

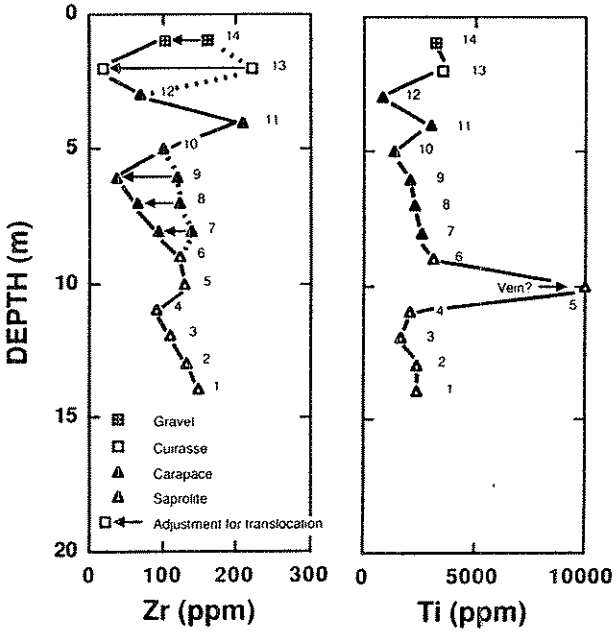

Fig. 8. Zr geochemical profile (left) corrected for zircon translocation (splid line) and uncorrected (dashed line) compared wit Ti profile (right). Zr analysis is by XRF on pressed pills and Ti is by AAS. Sample 5 contains a vein in the parent material which is enriched in Ti.

eq. (10). Notice that in general the resultant strain curves are similar in many respects: (1) large positive strains clearly indicated volume increase (expansion), (2) three distinct local strain maximas occur at about 2 to 7 and 12 m, and (3) strain appears to be decreasing from 12 m and deeper within the saprolite. Expansions indicated from the strain calculations are as high as 1, 2 or even more locally, corresponding to 100 or 200% increase in volume. Notice that samples 9 and 13, which are highly dilated, are also characterized by maximum development of clay films.

Besides destruction of lithostructure, further corroborative evidence for dilational strains can be seen in Fig. 10 which shows goethite pseudomorphs after pyrite in a state of dilation and separation by pedogenic material.

Internal consistency of strain from Zr and Ti

Reference elements, Zr and Ti can each be used in independent calculations of strain, and hence the internal consistency of the results can be ascertained by using Zr to evaluate Ti immobility and vice versa. Using the trans-

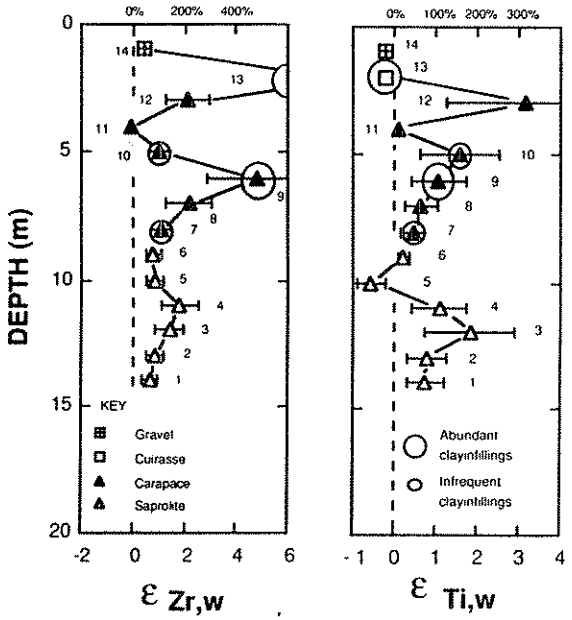

Fig. 9. Calculated strain profiles using Zr (left) and Ti (right). Error bars indicate variation using minimum and maximum values of strain index elements in parent material. A strain of 1 corresponds to 100% expansion.

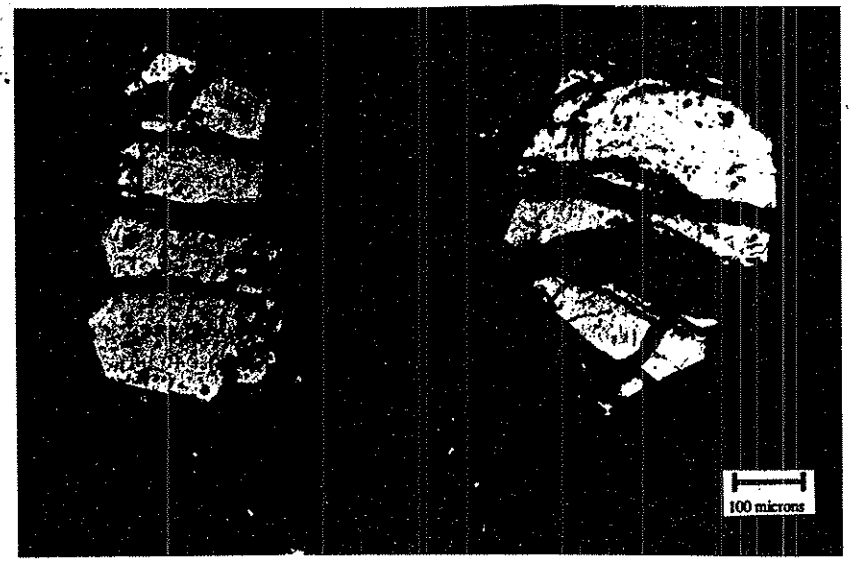

Fig. 10. Photomicrograph of expanded goethite pseudomorph after primary pyrite indicating state of local dilational strain.

location-corrected Zr data and bulk densities to compute strain, we calculate the mobility of Ti as its mobile mass fraction, $\tau_{Ti,\,w,\,\epsilon(Zr)}$ using eq. (8) (Fig. 11, left panel). In order to evaluate errors in this transport function and in strain, we have computed the maximum and minimum value of strain by using the extreme values of Zr concentration in the parent material. These extreme values are then used to compute extreme values in $\tau_{Ti,\,w,\,\epsilon(Zr)}$. Proof of immobility is established when some portion of the resultant line falls within the horizontal band formed by the protore samples. Using this error analysis, Ti appears to have been immobile except in samples 5, 9, and 13. Alternatively, using Ti as the strain marker, Zr appears to have been immobile in all samples, again except in samples 5, 9, and 13. Why this small subset of data appears to indicate local mobility of Zr and Ti, we are not certain. It is possible though, that the concentration of these elements in the protolith was sufficiently variable locally that the diamond drill core samples we used as parent material are not truly representative everywhere in the profile

INFLUX AND ACCUMULATION OF Al, Fe AND Si

Using the chemo-mechanical strain indicators offered by Zr and Ti, we now establish the extent of the mobility of Al, Fe, and Si, three of the major constituents in the laterite profile. Chemical profiles for these elements are shown in Fig. 12. In each case, erratic variation in the concentrations typify the data. However, when we compute the transport functions for each elements from eq. (8), the tau profiles which, besides depending upon chemical concentration, also include bulk density and strain, the profiles become much less erratic and smooth trends emerge. Figure 13 indicates influx and accumulation of Al, Fe, and Si in samples 9 and 13, a pattern which coincides exactly with the micromorphologic evidence of translocation of clays and Fe-oxides. Al and Fe translocation proceeds to greater depth than that of Si which ceases at about 10 m at the top of the saprolite. Within the saprolite, both Al and Fe have been introduced as indicated by positive tau values approaching 1 or 100% of the mass present in the parent material. It is vital to remember that tau refers to mass additions in excess of increases in concentration imparted by simple residual enrichment which results from reduction in bulk density as mobile elements are carried away.

Cumulative soils

The introduction and accumulation of Al, Fe, and Si provides new insight into the genesis of laterites that are not simply residual soils. It is necessary to view their chemistry as being strongly affected, if not dominated, by addition of material from above, from the top down to well within the saprolite. Cumulative soils; named by Nikiforoff (1949) receive influxes of "parent ma-

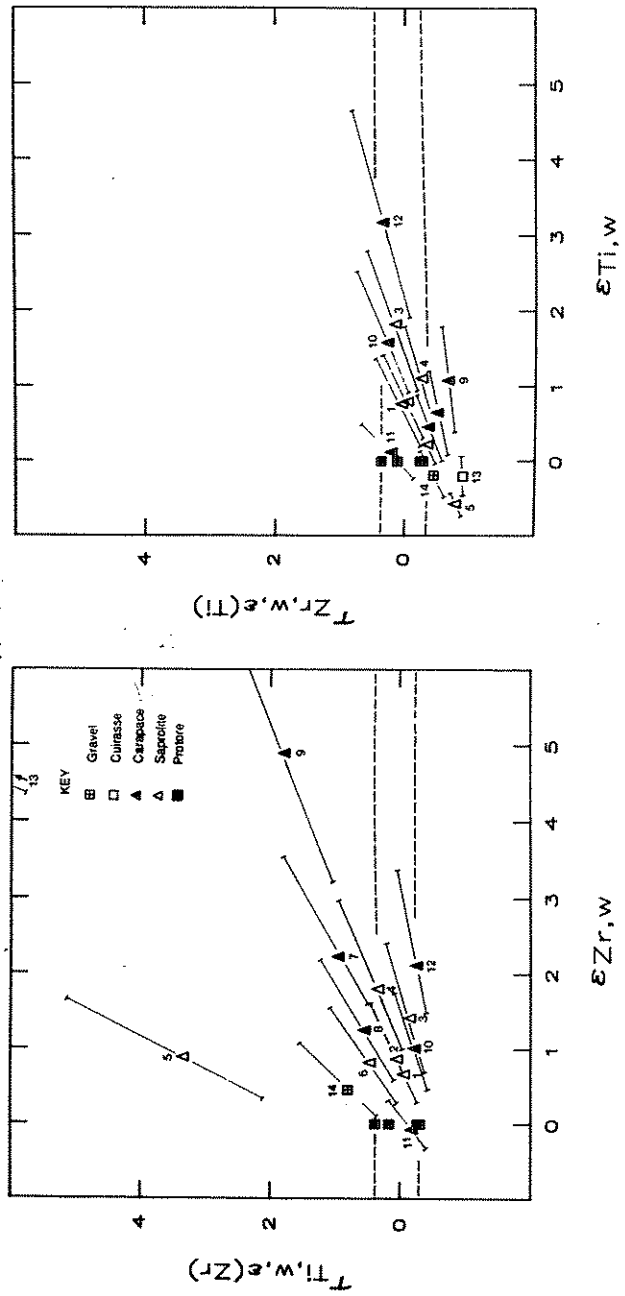

Fig. 11. Transported mass fraction of Ti versus strain computed by corrected Zr (left) and transported mass fraction of Zr versus strain computed by corrected Ti (right). Possible range of errors comes from using minimum and maximum concentration values of strain index elements in parent material. Dotted horizontal band shows this range. Proof of immobility then requires that the possible range for each sample. an inclined line centered on a mean sample value, should plot somewhere within the error envelope.

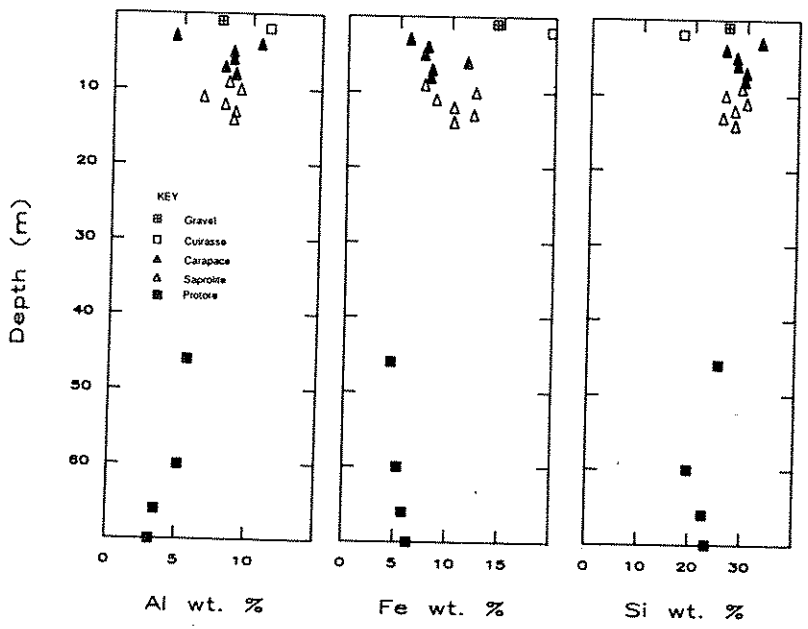

Fig. 12. Plain geochemical profiles for Al, Fe, and Si. Al and Fe analyses are AAS and Si is by XRF on glass plate cast from a fluxed melt of each sample.

terial" at the same time that soil formation is going on (Birkeland, 1974). Since cumulative soils have parent material added to their surfaces, they are partly sedimentologic and partly pedogenic. At Syama, it is apparent that the "parent material" being added is enriched in Al, Fe, and Si as well as in the mineral zircon. We infer therefore, that the added constituents consist of weathered material and is hence chemically mature. Given the position of Syama along the Harmatan dust trajectory stemming from the Sahara Desert, the foreign components may be a combination of eolian dust and chemically-mature detritus derived from the local regolith.

GEOCHEMICAL MECHANICS OF CUMULATIVE DILATION

Correlation of mass influx with strain

The vertical coincidence of dilated zones with translocation of Al, Fe, and Si, can ve evaluated critically by examining the correlation of transport functions, tau with strain. In Fig. 14 we show such plots for Al, Fe, and Si using both Zr and Ti as strain indicator in order to compare independent results. Two observations emerge from these correlations: (1) all three elements, Al

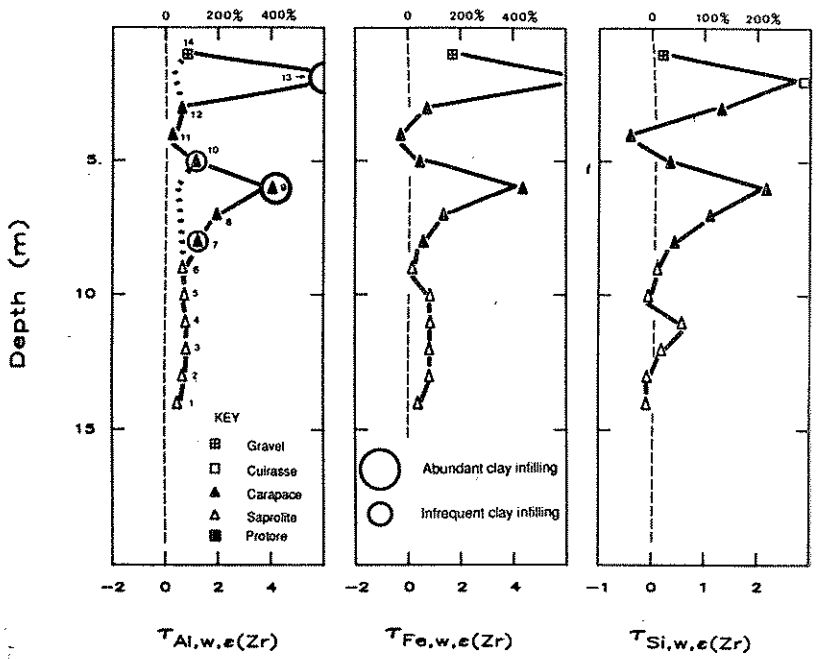

Fig. 13. Transported mass fraction tau profiles for Al, Fe, and Si. Solid line for Al is corrected for zircon translocation, dashed line is uncorrected. Notice intense mass accumulations of Al, Fe and Si at same sample depths as maximum development of clay infillings. A value of tau of plus 1 corresponds to addition of 100% of an element in excess of the mass originally present in the parent material. A value of 0 indicates only residual and deformational effects.

Fe, and Si have been added to the profiles, (2) their transport functions are directly correlated with net strain, that is, influx and accumulation increase as the extent of dilation increases. Correlation of influx with strain is real and is not simply a trivial consequence of the fact that introduction of Al, Fe, and Si minerals was accompanied by zircon influx because enrichment of Al, Fe, Si is correlative with dilations which are effectively a rarefaction of immobile elements rather than concentrating them.

An underlying reason for the correlation of strain with the accumulated mass fraction emerges in eq. (15) where the first term is simply the volume of the REV after weathering, V_w, which depends directly on the net sum of all the mass gains or losses of all the n elements in accord with their respective mass fractions, $\tau_{j,w}$. Recall that these functions are positive for elements added and negative for elements extracted from the profile:

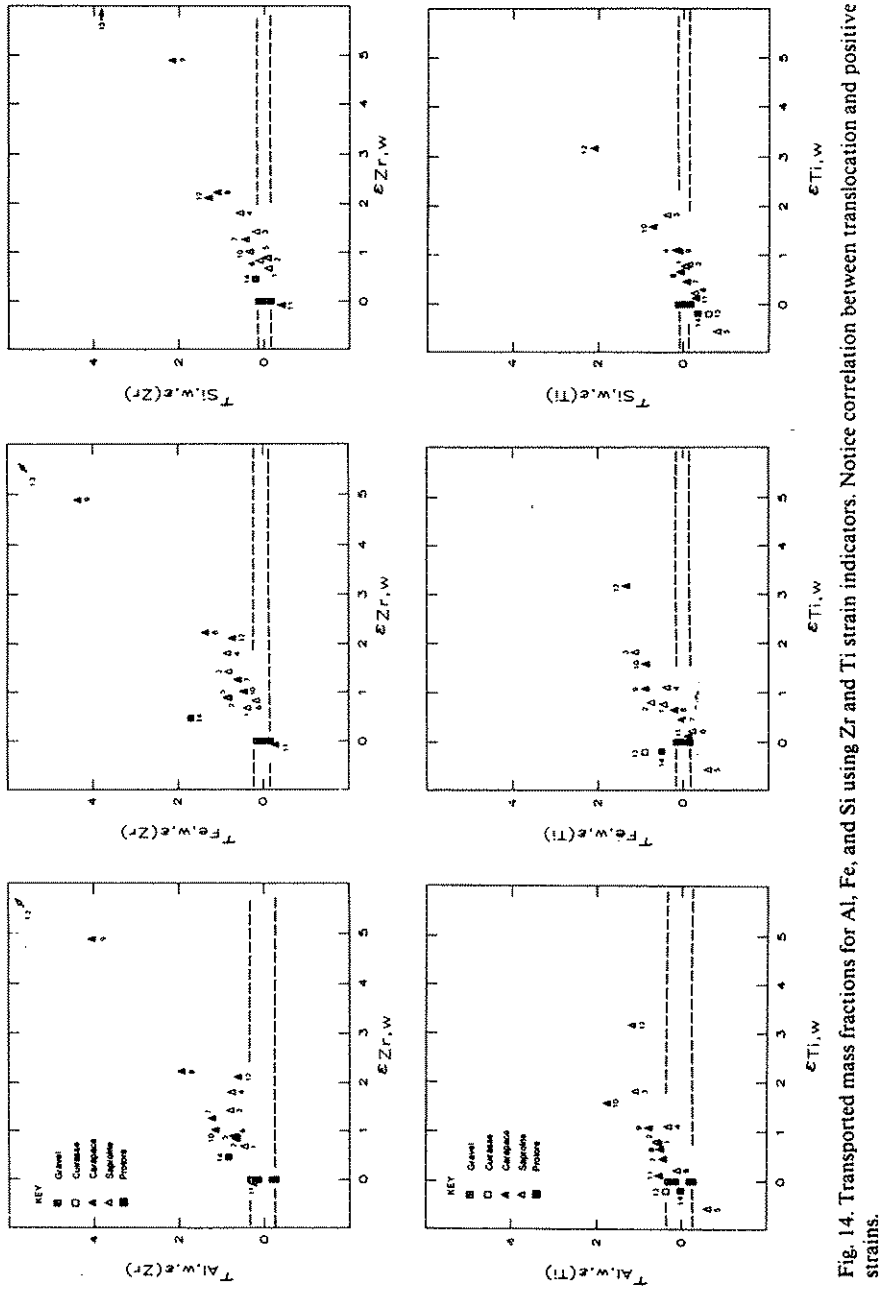

Fig. 14. Transported mass fractions for Al, Fe, and Si using Zr and Ti strain indicators. Notice correlation between translocation and positive strains.

$$\varepsilon_{i,\,w}=\left(\frac{\rho_p V_p+\sum_{j=1}^{n} m_{j,\,p}\tau_{j,\,w}}{\rho_w}\right)\left(\frac{1}{V_p}\right)-1 \qquad (15)$$

The form used in eq. (15), is equivalent to eq. (2). Clearly, mass additions can contribute to dilations and mass extractions can cause collapse as the sign of the individual transport functions, $\tau_{j,\,w}$ may be positive or negative. What dominates the accumulated strain is then the net accumulations or depletions.

While eq. (15) uses the dependence of volume on mass fluxes $\tau_{j,\,w}$, to illustrate how strains can be induced by translocation or dissolution, eq. (16), instead, emphasizes density changes which are given as total mass change summed over all mobile elements, n, per unit volume, V_p:

$$\varepsilon_{i,\,w}=\frac{1}{\rho_w}\left(\rho_p+\frac{\sum_{j=1}^{n} m_{j,\,p}\tau_{j,\,w}}{V_p}\right)-1 \qquad (16)$$

When this change in density, $\Delta\rho$, is added to the original density of the protolith, ρ_p, and the sum divided by the bulk density of the weathered product, ρ_w, yields a ratio different than unity, then with subtraction of 1, a non-zero strain results. Therefore, open-system mass transfer, viewed either as a *volumetric* or *densiometric* change, may produce significant accumulated strains in soils.

Chemo-biomechanical feedback model

We infer that a reciprocal or mutually reinforcing mechanical interaction between translocation of surficial detritus and deformation has occurred and the evidence lies in the observed micromorphological features and the spatial coincidence and proportionality of influx with dilational hyper-strains. The main issue to be resolved is then exactly how material influx is related to deformation. It is apparent that within the upper 8 m, the relatively high permeability indicates that voids are essentially connected above this transition to submicroscopic pores. Therefore, avenues for grain translocation may extend from the surface down to this critical depth. At least some of the voids are occupied by living roots, which have been observed to depths of 24 m. We propose that with progressive infilling of available voids, perhaps as roots decay and mineral dissolution occurs, accumulation of descending solids is so extensive that with subsequent root expansion, further root penetration, and or possible shrink-swell cycles, the combined soil skeleton and plasma cannot remain isovolumetric and incremental expansion occurs. Over an unknown amount of time, numerous generations of roots, and many seasons, strain accumulation occurs as the only means of relieving the increasing space

problem caused by continued translocation of mobile detritus or chemical precipitates into the subsurface.

We view translocated grains as serving the role of a mechanical wedge which infills vacant space and against which subsurface forces are exerted when root growth occurs. The combined effects of weathering, root growth, translocation, and deformation would appear to be a self-regulated, mutually-reinforcing process involving biomechanical feedback between root growth, translocation, and deformation. Cumulative microsedimentary infilling-structures contribute to the evolving soil texture, pedoturbation and evolution in chemical composition.

REGOLITH REDUCTION MODEL

Well-known landscape development models have existed (McFarlane, 1976; Fitzpatrick, 1980) describing weathering profile development by progressive replacement from a progenitor resembling that currently underlying it (Butt, 1983) as a process of chemical mass wasting which, in combination with slow physical erosion, lowers the landscape with time as much of the regolith becomes disaggregated and is removed from the surface by fluviatile action. We suggest here, instead, that subsurface storage and accumulation of local and foreign detritus may be an important contributing, if not dominant, factor in regional elevation. Rather than being lowered appreciably by erosion, perhaps the inferred open-system influxes and resultant dilations cause the surface to maintain a net long-term stability or even undergo an aggradation, though regolith reduction, escarpment retreat, and lateral transmigration unquestionably produce local topographic relief. The mobile element solute load of groundwater discharge departing from the saprolite column may be an important incipient stage of regolith reduction. In Fig. 15, we present a model for chemical and physical regolith reduction with a simultaneous influx of foreign and local sources of detritus.

Volume reduction

The usage of the term residual enrichment may cause confusion unless we clarify the term, "volume reduction" as it is commonly used. Jensen and Bateman (1981) refer to residual enrichment as accumulation of ore minerals when undesired constituents are removed during weathering with concentration due largely to a decrease in volume. Volume reduction can be traced back to Lindgren (1933) in describing gold enrichment in alluvial deposits in deeply-weathered terrains where he referred to mass loss as regolith reduction by removal of gangue mineral constituents. Here, because strain determination is possible, we may now distinguish residual enrichment from volume reduction. Residual enrichment results simply from change in bulk

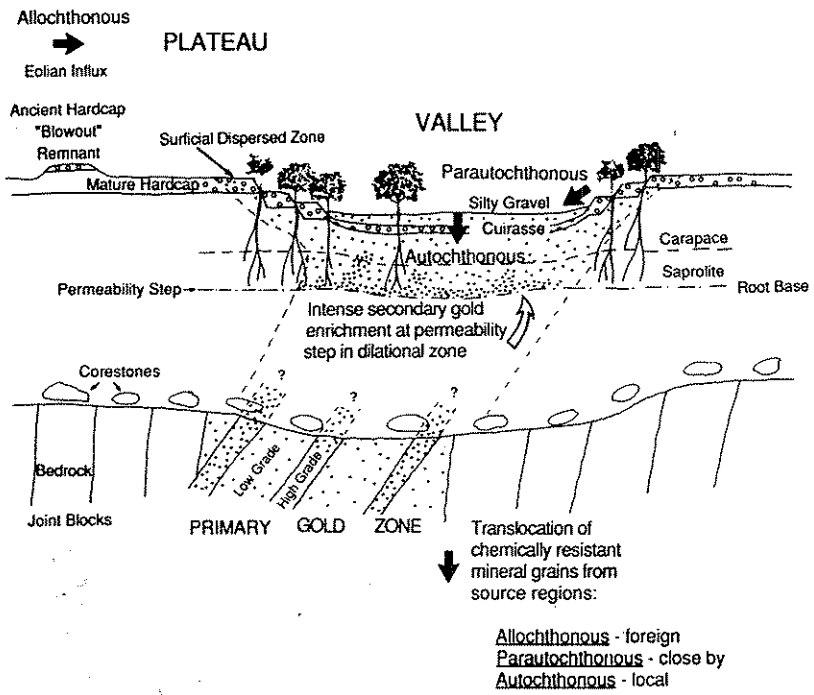

Fig. 15. Diagrammatic cross section showing sources of detritus, and mechanical supergene enrichment of gold particles.

density, ρ_p/ρ_w, as pores are created by dissolution of minerals and leaching of soluble constituents. It is separate and not necessarily accompanied by change in volume. If volume changes do occur, it is a strain. "Volume reduction" is then perhaps better viewed, not as a strain, but as a winnowing process causing a physical separation of constituents from the overlying horizons into two fractions: those which remain behind and are reincorporated into a soil profile below as mass influxes, and those which are simply removed. We propose that the term "volume reduction" be replaced by regolith reduction to avoid further confusion.

BEHAVIOR OF GOLD

We turn now to the behavior of gold in the laterite studied. It is important (1) because it is geochemically rare, it is clearly autochthonous; (2) because of its extremely high grain density (19 g/cm^3), in addition to its small size in relation to pore diameters, it undergoes little dispersion; and (3) it is vital to

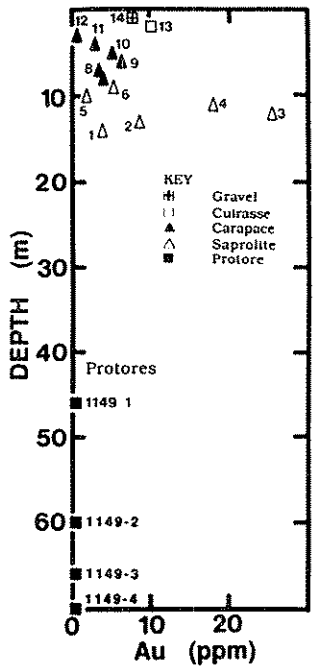

Fig. 16. Geochemical profile for Au. Analysis by fire assay on one meter channel samples of pit walls.

define mechanisms of gold enrichment in laterites and to relate its behavior to that of major elements to better understand the origin of an important new class of ore deposits. Application of mass balance techniques to gold geochemistry is a very difficult application, however, because of the variability of gold concentration in the parent material. This should be kept in mind in evaluating the results.

Gold profile and relation to strain

Figure 16 shows the geochemical profile of Au which has been used to compute the transport function of Au (Fig. 17, right panel) and which is correlated with the strain profile (Fig. 17, left panel). As with Al, Fe and Si, Au appears to accumulate in dilatant zones, especially in samples 9 and 13 where pore infillings are common. At greater depth than 12 m, Au also has accumulated, perhaps at the permeability step.

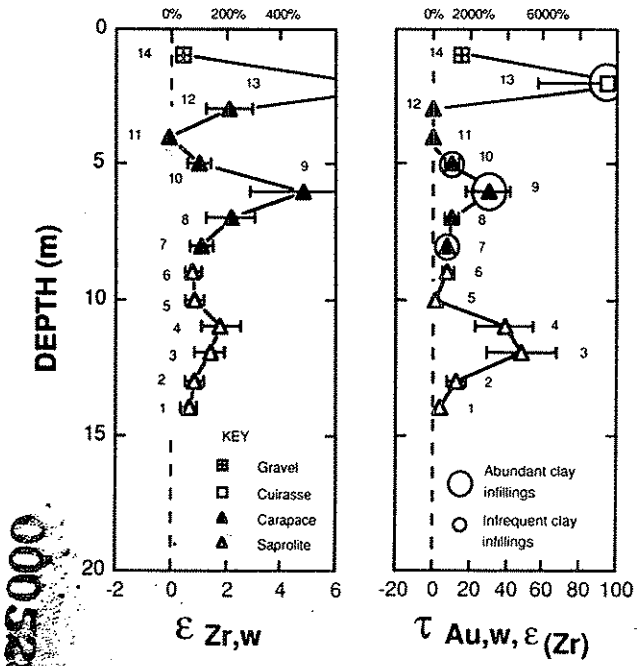

Fig. 17. Comparison of strain (left) with transported mass fraction of Au (right) showing spatial correlation of expansion with accumulation of gold by the proposed dilational regolith reduction model. Extremely high transported mass fractions in excess of 5000 result from the accumulation of very dense small particles of gold in the pore structures of the laterite as lateritic weathering progresses down through the gold-bearing parent material concentrating the captive gold in near-surface zones of maximum dilation.

Size and morphology of gold grains

To understand the transport and accumulation mechanism of Au shown in Fig. 17 (right panel), we have studied the size and morphology of gold grains in protore and weathered material by preparing concentrates. We do this by partially dissolving 10 g uncrushed samples. This helps ensure that the gold grains are not damaged mechanically by our preparation. The samples are placed in Teflon beakers and digested at room temperature by 25 ml of concentrated hydrofluoric acid and 5 ml of concentrated nitric acid. These acids are used to dissolve silicate minerals and more resistant phases as well while leaving gold grains relatively unaffected. When the acids are spent, we decant them and add new acids. Finally the resistate sludge is treated with a saturated boric acid solution to remove fluorides. These studies indicate that gold particles in the laterite are very similar in size to those already occurring in

the protore so there is little, if any, growth of gold grains during weathering. We interpret the size and shape data on gold grains to indicate that secondary gold enrichment was dominated by movement and concentration of gold particles present initially as microscopic inclusions in primary pyrite within the protolith rather than chemical dissolution and reprecipitation, although such chemical remobilization may have occurred to some extent locally.

CUMULATIVE SUPERGENE GOLD ENRICHMENT BY REGOLITH REDUCTION

We have seen no evidence for any type of transport except for gold particles migrating mechanically in solution in groundwater, although besides primary gold, electron microprobe analysis of pyrite indicates an appreciable invisible submicroscopic gold content which is liberated upon pyrite oxidation. Also we have not recognized any microscopic features which could be interpreted as evidence of chemical deposition from solution. This is borne out by the transport function profile for Au (Fig. 17, right panel) which is nowhere negative, implying that there is no possible source region within the present profile from which gold might have been locally derived. We therefore infer that gold migration by mechanical transport is a significant enrichment mechanism. We postulate then that the degraded regolith was the principal source region.

In Fig. 18 we envision an idealized sequence of steps in the weathering of a

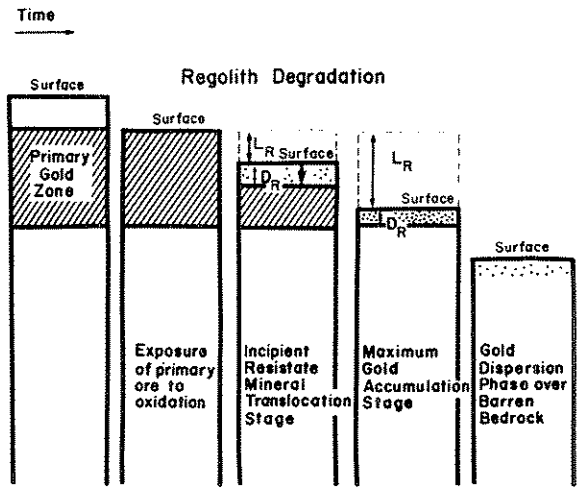

Fig. 18. Series of hypothetical cross sections showing evolution of lateritic gold anomaly as a primary gold zone is exposed to weathering, regolith reduction, and finally dispersal over barren bedrock with no primary gold.

bedrock zone of primary mineralization as degradation of the regolith proceeds. Once a primary gold anomaly is exposed to the weathering environment, electrum is essentially stable and is not removed from the system by erosion given its high grain density and small particle size. Instead, it simply accumulates selectively near the surface within a relatively shallow zone where it moves by translocation down through voids as the regolith is reduced. There is no remnant of the source region from which the gold has been derived.

Regolith reduction mass balance model

The proposed regolith reduction model is parameterized as follows: the depth to which translocation occurs is $D_{R_{j,p}}$ and the total vertical thickness of parent material which has undergone weathering to regolith which has been reduced is $L_{R_{j,p}}$ both given as lengths in their undeformed state. Overall mass balance of a chemically inert though not necessarily immobile mineral, leads to an enrichment factor equation:

$$\frac{C_{j,w}}{C_{j,p}}=\frac{1}{\varepsilon_{i,w}+1}\frac{\rho_p}{\rho_w}\left(1+\frac{L_{R_{j,p}}}{D_{R_{j,p}}}+\phi_{j,w}\right) \tag{17}$$

In eq. (17), the mass fraction added to a vertical profile undergoing regolith reduction from outside the column, say from lateral or eolian sources, is given in eq. (18) as $\phi_{j,w,ext}$ which is the ratio of mass added to that present initially in the protolith column:

$$\phi_{j,w,ext}=\frac{100m_{j,\text{ext flux}}}{D_{R_{j,p}}\rho_p C_{j,p}} \tag{18}$$

Since two sources of translocated elements are accounted for in eq. (17), the overall transport function, $\tau_{j,w}$ has two components: $L_{R_{j,p}}/D_{R_{j,p}}$ describing the translocation of autochthonous grains down through the vertical profile and $\phi_{j,w}$, allocthonous grains which describes influx of grains foreign to the profile, either nearby para-autochthonous or allocthonous detritus:

$$\tau_{j,w}=\frac{L_{R_{j,p}}}{D_{R_{j,p}}}+\phi_{j,w} \tag{19}$$

$L_{R_{j,p}}/D_{R_{j,p}}$ has a focussing effect on translocated grains; the greater the thickness of protolith reduced or the smaller the depth of accumulation of translocated grains, the greater the value of the transport function. Regolith reduction is imply a mechanical lens which selectively removes certain elements, and concentrates others effectively.

When the influx of foreign material is negligible, eq. (19) can be reduced and solved for estimate of the vertical column height of protolith which underwent weathering and regolith reduction:

$$L_{R_{j,p}}=D_{R_{j,p}}\tau_{j,w} \tag{20}$$

The various sources of gold and other resistate constituents are represented diagrammatically in Fig. 15. Here we show gold in the protore being enriched above the bedrock–saprolite interface at a depth of maximum translocation of gold particles: (1) *autochthonous* coming from local downward transport of gold within a weathering profile, (2) *parautochthonous* coming from nearby but not vertically above, and for elements other than gold, (3) *allochthonous* coming from foreign sources such as eolian dust particles or from fluviatile transport over substantial distances.

CONCLUSIONS

Using a quantitative strain meter, we demonstrate that local dilations in excess of 200 and even 300% of the initial volume have occurred. Intensely dilated samples also have maximum development of clay infillings and maximum values of transported mass fraction of chemically-mature, Fe- and Al-rich autochthonous and parautochthonous detritus derived by reduction of the regolith column and soil mantle. We propose that the coincidental dilations and mass influx of Al, Fe, and Si result from a reciprocal, mutually reinforcing, mechanical interaction between translocation and deformation by root expansion or shrink-swell cycles. Continued microsedimentary infilling causes a space problem resolved only by expansion. Relaxation or reversion to an unstrained state is impossible because of continued cyclic translocation, void infilling and root growth acting as a growing wedge of accumulating detritus in the subsurface. Escarpment retreat and regolith reduction release resistates which are locally transported, recycled and volumetrically focussed in the permeable near-surface environment to a depth limited by the relative size of mineral particles and connected pores. Inversion of the landscape occurs as old duricrust mesas are degraded and new ones develop in nearby topographic depressions from recycling of detritus. Lateral dispersion of elements, such as gold, which come from the local parent material is thereby minimized.

With this study we have gained a clearer glimpse of exactly what role residual enrichment plays in laterite development. Residual enrichment in a lateritic weathering profile, is simply due to density changes, and by eq. (14) is given by ρ_p/ρ_w which has a maximum value of 2.6. It is best viewed as an ongoing in situ modification of parent material which has an increasingly-eclectic character near its top because of increased levels of contamination by surficial detritus retained locally because of the relatively low erosion rates on tectonically-stable cratons and the unusually important role of dust deposition in such areas. Overall then, residual enrichment dominates only the basal saprolitic portions of laterites, where influx is minimal. Higher up above the saprolite, the accumulated effects of mineral translocation of detritus of local

and foreign derivation, as indicated by transported mass fraction in excess of 4 (Fig. 13), dominate the bulk chemistry of many samples as reflect the abundance of infilled pores. The upper portion of the profile may itself be the source region of detritus moving further along a dust trajectory. The migration of surficial detritus into the ocean basins is thereby delayed and widespread cumulative lateritic soils become the long-term repositories of an aged continental residuum.

The principal variables of interest in cumulative supergene gold enrichment are (1) the amount of protore weathered to form regolith which then undergoes reduction in mass and volume, and (2) the depth to which translocation of detritus from the degrading regolith occurs. These two factors are expressed as the ratio of the vertical height of protore affected by chemical weathering divided by the depth of secondary enrichment. This has a volumetric focussing effect and works as a chemical lens taking gold from a large source region and redepositing it in a smaller volume in an enriched state. Perhaps the most significant controlling physical variables on the depth to which significant translocation of Au, Al, Fe, and Si occurs is hydraulic conductivity. In the pit studied, hydraulic conductivity decreases by three orders of magnitude (a factor of 1000) within the upper part of the saprolite. This step in permeability may relate to depth of common modern tree rooting, which may be responsible for generating tubules exploited by translocation.

Finally, we are working towards establishing a standard set of essential chemical and physical measurements which are scaled automatically to characteristics of parent materials by constitutive mass balance relations. Such an analytical description of soils lends itself to the formulation of steady-state and dynamic models (Alpers and Brimhall, 1988, 1989) and to their testing by design and implementation of numerical computer simulations of chemical mass transport and kinetics following on developments of Helgeson (1968 and 1971) and more recent attempts to couple chemical reaction with ground water fluid flow (Ague and Brimhall, 1989).

ACKNOWLEDGEMENTS

This paper has benefited from reviews by Gary Sposito and especially from careful and insightful comments from Ron Amundson and Oliver Chadwick who helped us greatly in articulating our efforts to bridge the divergent perspectives between pedology, geochemistry, and economic geology. We gratefully acknowledge the support of NSF grants EAR-8804136 and EAR-8416790, which, in combination with research funding and logistical support in Africa from BHP-Utah International Minerals, made the theoretical, field and laboratory work of this project possible. Kathy Danti performed electron microprobe analyses on Syama minerals assisted by John Donovan who made technical upgrades to do trace element analyses. Collaboration, constructive criticism and on-going dialogue with William Dietrich, Ambogo Guindo, Fabrice Colin, Paolo Vasconcellos, Robin Fiebelkorn, Demetrius Pohl and Chris Carlson is much appreciated. Tim Teague prepared thin sections from impregnated soil samples, which made micromorphology possible. Joachim Hampel performed X-ray fluorescence analysis which was invaluable to strain determination. Dave Smith prepared sampling supplies for the field work.

REFERENCES

Ague, J. and Brimhall, G.H., 1989. Geochemical modeling of steady state fluid flow and chemical reaction during supergene enrichment of porphyry copper deposits. Econ. Geol., 84: 506–528.

Alpers, C.N. and Brimhall, G.H., 1988. Middle Miocene climatic change in the Atacama Desert, northern Chile. Evidence from supergene mineralization at La Escondida: Geol. Soc. Am., 100: 1640–1656.

Alpers, C.N. and Brimhall, G., 1989. Paleohydrologic evolution and geochemical dynamics of cumulative supergene metal enrichment at La Escondida, Atacama desert, Northern Chile. Econ. Geol., 84: 229–255.

Barshad, I., 1964. In: F.E. Bear (Editor), Chemistry of the Soil. Reinhold, London.

Birkeland, P.W., 1974. Pedology, Weathering, and Geomorphological Research. Oxford University Press, New York, 285 pp.

Boyle, R.W., 1979. The Geochemistry of Gold and Its Deposits, Bull. Geol. Surv. Can., 280: 584 pp.

Brimhall, G.H., 1987. Preliminary fractionation patterns of ore metals through earth history. Chem. Geol., 64: 1–16.

Brimhall, G.H. and Dietrich, W.E., 1987. Constitutive mass balance relations between chemical composition, volume, density, porosity, and strain in metasomatic hydrochemical systems: results on weathering and pedogenesis, Geochim. Cosmochim. Acta, 51: 567–587.

Brimhall, G.H. and Rivers, M.L., 1985. Semi-automated optical scanning device. United States Patent Number 4,503,555.

Brimhall, G.H., Alpers, C and Cunningham, A.B., 1985. Analysis of supergene ore-forming processes using mass balance principles. Econ. Geol., 80: 1227–1254.

Brimhall, G.H., Lewis, C.J., Ague, J.J. Dietrich, W.E., Hampel, J. and Rix, P., 1988. Metal enrichment in bauxites by deposition of chemically mature aeolian dust. Nature, 333: 819–824.

Brimhall, G.H., Lewis, C.J., Taylor, G., Ford, C. and Bratt, J., 1989. Cumulative supergene chemomechanical enrichment of Au, Al, Fe, Mo, Pb, and V by regolith reduction with grain translocation and soil hyperstrain in laterites in Mali, West Africa (Abstr). Intern. Geol. Congr., 1: 201.

Butt, C.R.M., 1983. Weathering and the Australian landscape. In: R.E. Smith (Editor), Geochemical Exploration in Deeply Weathered Terrains. CSIRO, Wembley, W. A., pp. 41–50.

Cumberlidge, J.T. and Chase, M.C., 1968. Geology of the Nickel Mountain Mine, Riddle, Oregon. In: J.D. Ridge (Editor), Ore Deposits of the United States, 1933–1967. Graton–Sales Volume. Am. Inst. Mining and Metall. Petrol. Engineers, New York, 2, pp. 1650–1672.

Davy, R., 1979. A study of laterite profiles in relation to bed rock in the Darling Range near Perth, W.A., Rep. No. 8, Geol. Surv. Western Australia, 87 pp.

Davy, R. and El-Ansary, M., 1986. Geochemical patterns in the laterite profile at the Boddington Gold Deposit, Western Australia. J. Geochem. Explor., 26: 19–144.

Derry, D.R., 1980. A concise Atlas of Geology and Mineral Deposits. Mining Journal Books, Halstead Press, London, 108 pp.
De Witt, M., Jeffrey, M., Bergh, H. and Nicolaysen, L., 1988. Geological Map of Gondwana. Am. Assoc. Petrol. Geologists.
Dixon, C.J., 1979. Atlas of Economic Mineral Deposits. Cornell Univ. Press, Ithaca, NY, 143 pp.
El-Baz, F. and Hassan, M.H.A., 1986. Physics of Desertification. Martinus Nijhoff, Dordrecht, 473 pp.
Esson, J., 1983. Geochemistry of a nickeliferous laterite profile, Liberdale, Brazil. In: R.C.L. Wilson (Editor), Residual Deposits: Surface Related Weathering Processes and Material. Blackwell, Oxford, pp. 91–102.
Fitzpatrick, E.A., 1980. Soils, their Formation, Classification and Distribution. Longman, London, 353 pp.
Goudie, A., 1973. Duricrusts in Tropical and Subtropical Landscapes. Clarendon Press, Oxford, 174 pp.
Goudie, A.S., 1983. Dust storms in space and time. Prog. Phys. Geogr., 7: 502–530.
Golightly, J.P., 1981. Nickeliferous laterite deposits. In: B.J. Skinner (Editor), 75th Anniversary Volume. Econ. Geol., 75: 710–734.
Helgeson, H.C., 1968. Evaluation of irreversible reactions in geochemical processes involving minerals and aqueous solutions. I. thermodynamic relations. Geochim. Cosmochim. Acta, 32: 853–877.
Helgeson, H.C., 1971. Kinetics of mass transfer among silicates and aqueous solutions. Geochim. Cosmochim. Acta, 35: 421–469.
Hotz, P., 1964. Nickeliferous laterites in southwestern Oregon and northwestern California. Econ. Geol., 59: 355–397.
Jensen, M.L. and Bateman, A.M., 1981. Economic Mineral Deposits. Wiley, New York, 214 pp.
Lelong, F., Tardy, Y., Grandin, G., Trecases, J.J. and Boulange, B., 1976. Pedogenesis, chemical weathering, and processes of formation of some supergene ore deposits. In: K.H. Wolf (Editor), Handbook of Stratabound Ore Deposits, 3. Elsevier, Amsterdam, pp. 93–173.
Lindgren, W., 1933. Mineral Deposits., McGraw-Hill, New York, pp. 219–220.
Mann, A.W., 1983a. Hydrogeochemical facies and regimes of South Australia. In: R.E. Smith (Editor), Geochemical Exploration in Deeply Weathered Terrain. CSIRO Inst. Energy and Earth Resources, Wembley, pp. 158–167.
Mann, A.W., 1983b. Hydrogeochemistry and weathering on the Yilgarn Block, Western Australia-ferrolysis and heavy metals in continental brines. Geochim. Cosmochim. Acta, 47: 181–190.
Mann, A.W., 1984. Mobility of gold and silver in lateritic weathering profiles: Some observations from Western Australia, Econ. Geol., 79: 23–37.
McFarlane, M.J., 1976. Laterite and Landscape. Academic Press, London, 151 pp.
Moraless, Ch. (Editor), 1979. Saharan Dust — Mobilization, Transport, Deposition. Wiley, New York, 316 pp.
Nikiforoff, C.C., 1949. Weathering and soil evolution. Soil Sci., 67: 219–223.
Nahon, D., 1989. Chemical lateritic weathering: 28th Int. Congr. (Abstr.), 2: 490.
Pye, K., 1987. Aeolian Dust and Dust deposits. Academic Press, London, 334 pp.
Pye, K., 1988. Bauxites gathering dust. Nature, 333: 800.
Samama, J.C., 1986. Ore Fields and Continental Weathering. Van Nostrand Reinhold, New York, 326 pp.
Smith, R.E. (Editor), 1983. Geochemical Exploration in Deeply Weathered Terrain. CSIRO, Wembley, W. A., 266 pp.
Stallard, R., 1989. Weathering processes and chemical composition of tropical rivers from diverse tectonic settings. 28th Int. Congr. (Abstr.), 3: 169.

Tardy, Y. and Nahon, D., 1985. Geochemistry of laterites, stability of Al-goethite, Al-hematite, and Fe^{3+}-kaolinite in bauxite and ferricretes: an approach to the mechanism of concretion formation. Am. J. Sci., 285, 865–903.
Valeton, I., 1983. Palcoenvironment of lateritic bauxites with vertical and lateral differentiation. In: R.C.L. Wilson (Editors), Residual Deposits: Surface Related Weathering Processes and Material. Blackwell, Oxford, pp. 77–90.
Velbel, M.A., 1985. Geochemical mass balances and weathering rates in forested watersheds of the southern Blue Ridge. Am. J. Sci., 285: 904–930.
Webster, J.G. and Mann, A.W., 1984. The influence of climate, geomorphology and primary geology on the supergene migration of gold and silver. J. Geochem. Explor., 22: 21–42.
Yaalon, D.H., 1987. Saharan dust and desert loess: effect on surrounding soils. J. Afr. Earth Sci., 6(4): 569–571.